Journal of Applied Polymer Science

Cellulose NANOFIBER-polyethylene nanocomposites modified by polyvinyl alcohol

Alper Kiziltas,[1,2] Behzad Nazari,[3] Esra Erbas Kiziltas,[1,4] Douglas J. S. Gardner,[1,4] Yousoo Han,[1] Todd S. Rushing[5]

[1]Advanced Structures and Composites Center (AEWC), University of Maine, Orono, Maine 04469
[2]Department of Forest Industry Engineering, Faculty of Forestry, University of Bartin, Bartin, 74100, Turkey
[3]Department of Chemical Engineering, University of Maine, Orono, Maine 04469
[4]The Scientific and Technological Research Council of Turkey (TUBİTAK), Tunus Cad, Kavaklıdere, Ankara 06100, Turkey
[5]U.S. Army Engineer Research and Development Center, 3909 Halls Ferry Road, Vicksburg Mississippi 39180
Correspondence to: A. Kiziltas (E-mail: kiziltasalper@gmail.com)

ABSTRACT: The uniform dispersion of cellulose nanofibers (CNFs) in non-polar polymer matrices is a primary problem to overcome in creating novel nanocomposites from these materials. The aim of this study was to produce CNF-polyethylene (PE) nanocomposites by melt compounding followed by injection molding to investigate the possibility of using polyvinyl alcohol (PVA) to improve the dispersion of CNF in the PE matrix. The tensile strength of CNF- filled composites was 17.4 MPa with the addition of 5 wt % CNF–PVA, which was 25% higher than the strength of neat PE. The tensile modulus of elasticity increased by 40% with 5% CNF–PVA addition. Flexural properties also significantly increased with increased CNF loading. Shear viscosity increased with increasing CNF content. The elastic moduli of the PE/CNF composites from rheological measurements were greater than those of the neat PE matrix because of the intrinsic rigidity of CNF. Melt creep compliance decreased by about 13% and 45% for the composites with 5 wt % CNF and 10 wt % CNF, respectively. It is expected that the PVA carrier system can contribute to the development of a process methodology to effectively disperse CNFs containing water in a polymer matrix. © 2015 Wiley Periodicals, Inc. J. Appl. Polym. Sci. **2016**, *133*, 42933.

KEYWORDS: cellulose and other wood products; manufacturing; rheology; thermogravimetric analysis; thermoplastics

Received 24 May 2015; accepted 15 September 2015
DOI: 10.1002/app.42933

INTRODUCTION

Cellulose nanofibers (CNFs) have great potential as reinforcement in polymer nanocomposites because of their superior mechanical properties, nanoscopic size, abundance, low weight, renewability, biodegradability, nontoxicity, and biocompatibility.[1–3] Therefore, CNFs have been extensively researched around the world, and the number of publications including research papers and patents on the preparation of nanocomposites containing CNFs has increased in recent years.[4–8] A broad range of potential applications of CNF to high-performance bio/nanocomposites have been developed, and these applications are expected to open up opportunities for the replacement of conventional petroleum-based composites with new and improved materials.[1,2,9] However, despite the attractive properties of CNFs, there are several obstacles to their use including lack of cost-effective production methods, difficulty of dispersion in non-polar matrix systems and non-aqueous media, and inadequate interfacial adhesion properties.[2,3]

The degree of dispersion of CNFs in a thermoplastic matrix strongly depends on the conditions of the melt compounding and processing techniques, such as extrusion or injection molding, used to prepare the CNF-reinforced polymer composites.[1,10] CNF dispersion in a thermoplastic can be limited by the processing temperature, which is restricted to about 200°C with CNFs, and the incompatibility between hydrophilic CNFs and hydrophobic thermoplastics.[2,10–12] There are many publications based on cellulose nanocomposites; however, there have been relatively few reports on studies using CNFs with hydrophobic thermoplastics such as polypropylene (PP), polyethylene (PE), and polystyrene (PS). CNF reinforcement of hydrophobic thermoplastic polymers has received far less attention than water soluble polymers or latexes as matrix resins for CNFs. Some reported examples of polyolefin (PP and PE)-based nanocomposites reinforced with CNFs are summarized in Table I.

Melt compounding was chosen over solvent casting for this study because melt processing is more practical for scaling up

Table I. Polyolefin Based Nanocomposites Processed for CNFs (Modified from Dufresne[10])

Polymer	Type of nanocellulose	Processing aid/Surface modification	Processing method	Characterization method	Reference
PE	CNF	DOPE Process	Extrusion/ Microcompounder	Fluorescence Spectroscopy, UV-Vis, LSCM and SEM	13
	CNC	Polyoxyethylene (PEO)	Extrusion	Rheology, SEM, TGA	1
	CNC	Aliphatic Chain Grafting (Hexanoyl, Lauroyl, and Stearoyl Chloride)	Extrusion/Micro-compounder (Twin Screw)	TEM, FTIR, XPS, XRD, EA, CA, TGA, DSC, DMA and Tensile Test	14
	CNC	Acetone (Gel Procedure) and MAPE	Brabender/Compression Molding	Tensile Test, FTIR and AFM	15
	MFC	Ethylene–Acrylic Oligomer Emulsion	Brabender/Compression Molding	Tensile Test, TEM, XRD and SEM	16,17
PP	MFC	Ethanol Swelled MFC	Melt Mixer/Compression Molding	SEM, XRD, DSC and Tensile Test	18
	MFC	Ethylene–Acrylic Oligomer Emulsion	Brabender/Compression Molding	Tensile Test, TEM, XRD and SEM	16
	MFC	Carrier Systems (Thermoplastic Starch)/ MAPP/Surfactants	Brabender/Injection Molding	Tensile, Flexural and Impact Tests, SEM, DSC and TGA	19,20
	CNF	Polycaprolactone (PCL) and Kneading Process	Kneading/Compression Molding	SEM, AFM, Tensile Test and DSC	2
	CNF and MFC	-	Brabender/Injection Molding	Tensile, Flexural and Impact Tests, TGA, Fracture Initiation Resistance Theory and SEM	21–26
	CNW	Toluene/MAPP/Non-Polar Solvent	Solvent Casting/Hot Press/Film Preparation	Tensile Test, SEM, XRD, DSC, DMA	27,28
	RSNF	MAPP	Extrusion/Hot Press	Tensile Test, SEM and FTIR	29
	CNC	MAPP/Nanoclay	Extrusion/Injection Molding	FTIR, DSC, TGA, XRD, SEM, TEM and Tensile Test	12
	CNW	MAPP/Toluene	Solvent Casting/Hot Press/Film Preparation	SEM, FTIR, Tensile Test, DSC, TGA, CA, DMA and Thermal Conductivity	3,30
	CNC	MAPP, CTAB, Acetylation and Fractionation	Solvent Casting/ Extrusion	TEM, Tensile Test, Raman Analysis and Mapping.	31

to an industrial level. Several routes were explored to improve compatibility at the fiber–matrix interface and to enhance dispersion of CNFs that included use of surfactants, use of functionalized CNFs, and use of coupling agents; however, these strategies can be expensive, time consuming, and impractical in industrial applications.[1,12,32] A possible approach to obtain better CNF dispersion in a hydrophobic thermoplastic is to use a water soluble polymer as a carrier for CNFs. Water soluble polymers are expected to encapsulate single CNFs, providing better dispersion in the polymer matrix and formation of strong hydrogen bonds as the water is evaporated.[33] Kiziltas *et al.* studied the possibility of using thermoplastic starch as a carrier system for unmodified and modified CNF suspensions in a PP matrix. They found that the flexural modulus and strength of the composites increased compared to neat PP matrix with modified CNF suspensions.[19,20] Poly(vinyl alcohol) (PVA) is a high strength, water soluble polymer produced in large volumes and should be a candidate carrier system for CNFs in hydrophobic polymers. Bondeson and Oksman produced PLA/cellulose nanowhiskers (CNW) nanocomposites by compounding extrusion and investigated the possibility of using PVA to uniformly disperse the CNW in the PLA matrix. The PLA, PVA, and CNW (dry and wet) content in the formulations studied were 65, 30, and 5 wt %, respectively.[33]

The objective of the present study was to use PVA to create compatibility between the CNF suspension and a conventional PE matrix, and to increase the mechanical properties of PE using CNF with PVA. In this study, the PE composites were prepared by melt blending followed by injection molding. Tensile, flexural, and impact tests were performed to evaluate the mechanical properties of the composites. The composite morphologies were studied using a scanning electron microscope (SEM). Rheological behavior including elastic modulus and viscosity of PE composites was determined by a stress-controlled Bohlin Gemini rheometer.

EXPERIMENTAL

Materials

The high-density PE used as the thermoplastic matrix polymer was supplied by Equistar Chemical Co., USA. This PE had a density of 0.95 g/cm^3 and a MFI of 5.0 g/10 min. at 190°C. The melting temperature was 128°C, and the crystallization temperature was 113°C as reported by the manufacturer. A partially hydrolyzed PVA was supplied by Sekisui Specialty Chemicals America, LLC. USA. The glass transition temperature (T_g) was 58°C, and the density was 1.27–1.31 g/cm^3 based on information from the supplier. CNF, trade name Celish-Rokameijin, was supplied by Daicel Chemical Industries, Ltd., Japan. This product consisted of a 35 wt % fiber content slurry.

Processing of Composite Materials

The authors observed that dispersion of CNF in PE was more difficult as compared to the PVA matrices. Therefore, CNF was pre-compounded with PVA. Then the obtained material (PVA/CNF) was blended with the PE during a second compounding step. Table II lists the compositions of the nanocomposites prepared in this study. The CNF suspension was first mixed with PVA at contents of 10, 25, and 50 wt % CNF using a Brabender Prep-mixer® equipped with a bowl mixer at 180°C and 60 rpm. No pre-drying of the CNF was required for compounding. After processing, the CNF–PVA mixture was cooled and cut into small particles to be premixed with the PE matrix. The CNF–PVA mixtures and PE were dried to a moisture content of less than 1%. The moisture information obtained according to ASTM D5229M-14. PE was melt compounded with CNF, neat PVA, and CNF–PVA mixtures. CNF, PVA, and CNF–PVA mixtures were added to the mixer (Brabender Prep-mixer®) when the PE melt appeared well mixed at 180°C and 60 rpm. After the compounding, the PE and composites were cooled and granulated using a laboratory-scale grinder. The ground particles were dried in an oven at 80°C in preparation for injection molding. All test specimens, which were made according to ASTM standards, were injection molded using a barrel temperature of 180°C, a mold temperature of 180°C, and an injection pressure of 2000 psi.

Characterization

Tension, flexural and notched Izod impacts tests were conducted according to the American Society of Testing and Materials (ASTM) standard D 638-03 Type I, ASTM D 790-03, Test Method 1, Procedure A, i.e., three-point loading system utilizing center-point loading and ASTM D 256-06 respectively. These mechanical testing was detailed in Aydemir *et al.* and Ozen *et al.*[34,35] Thermal stability of the composites was examined by thermogravimetric analysis (TGA) and the TGA testing is detailed in Kiziltas *et al.*[36] Rheological properties of the PE and CNF composites were measured by a stress-controlled rheometer at a temperature of 190°C. Details of rheological measurements can be found Kiziltas *et al.*[36] Creep recovery tests were also performed in the rotational mode of the rheometer at a temperature of 190°C and a constant stress of 200 Pa. The stress was removed after 60 s, and strain recovery was recorded. The rheological behavior of the composites was also studied using an MFI tester at a temperature 180°C and the MFI testing is detailed in Aydemir *et al.*[37] Hitachi-TM 3000 table top microscope at an acceleration voltage of 15 kV was used to determine the dispersion and the quality of the interfaces between the CNFs and the PE matrix from the facture surfaces of the composites after impact testing.

Table II. Composition of PE, PE+PVA, and CNF Composites

Sample Code	PE	PVA	CNF
PE	100	0	0
PE+PVA	90	10	0
1% CNF	90	9	1
2.5% CNF	90	7.5	2.5
5% CNF	90	5	5
10%CNF	90	0	10

Values are percentage by weight (wt %).

Statistical Analysis

The mechanical properties and MFI values were compared using a one-way analysis of variance followed by a Tukey-Kramer Honestly Significant Differences (HSD) test using the JMP statistical analysis program.[38]

RESULTS AND DISCUSSION

Thermal Properties

TGA and derivative TGA (DTGA) curves for the neat PE, PVA, CNF, and composites are shown in Figure 1. For the neat CNF, three stages of mass loss were observed. A first stage, up to 200°C, corresponded to less than 4 wt % loss and was followed by a second stage with more than 85 wt % loss up to about 400°C. The third stage extended to the usual ending test temperature at 600°C with more than 89 wt % loss. The weight loss at 100°C was only 3.2%, and at 250°C was 3.7%. The total weight loss at 600°C was 89.7%, which showed that only 10.3% was the residue present in the CNF. Similar to CNF, three stages of mass loss were observed in the TGA curve for neat PVA. A first stage, up to 200°C, corresponded to less than 2 wt % loss, and was followed by second stage with more than 65 wt % loss, up to 300°C. The initial loss, below 200°C is usually associated with the release of water or other volatiles from the PVA.[39] The second stage was associated with dehydration reactions.[40] The third stage occurred above 400°C and involved the decomposition of carbonaceous matter.[41] The weight loss at 100°C was only 0.7%, and at 250°C was 14.9%. The total weight loss at 600°C was 91.3%, which showed that only 8.7% was the residue present in the PVA. The degradation temperatures of the PE,

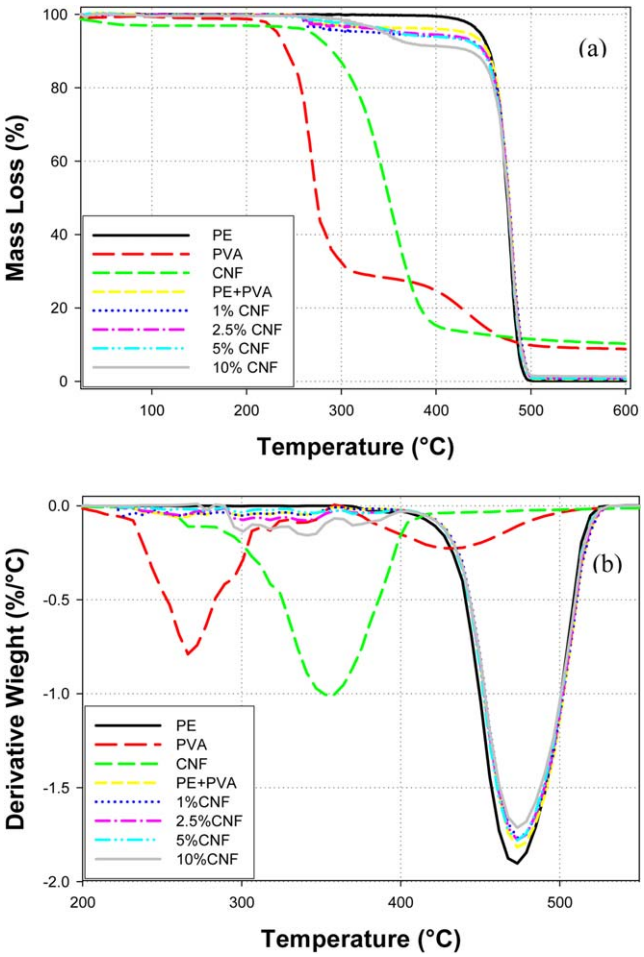

Figure 1. (a) TGA and (b) derivative TGA curves of neat PE, PVA, CNF, and composites from room temperature to 600°C. [Color figure can be viewed in the online issue, which is available at wileyonlinelibrary.com.]

PE+PVA, and CNF composites were different in Figure 1(b). The results also showed that the thermal stability of the composites decreased slightly as the CNF content increased because of the lower thermal stability of CNF compared to the neat PE.

Mechanical Properties

The results of mechanical property measurements of the composites are presented in Table III. Neat PE exhibited a typical yielding process and ductile nature followed by strain hardening with a tensile strength of 13.9 MPa. All composites including PE+PVA showed signs of stress yielding. Generally, a reduction of tensile strength was expected after the mixing cellulose fillers into hydrophobic matrices caused by incompatibility between hydrophilic cellulose and hydrophobic matrices, but the CNF-reinforced composites with PVA as a carrier system displayed enhanced tensile properties compared with the neat PE in this study.[1,10] Due to better compatibility as well as better stress-transfer properties, tensile strength of the composites was greater (increasing by 25% to 17.4 MPa with the addition of 5% CNF).[35,42]

TMOE of the composites continuously increased with increasing CNF loading (increasing by 40% to 1.1 GPa with the addition of 5% CNF). The increase in TMOE is a common trend according to previous research results for cellulose nanofibrils.[43,44] Significant property differences between composites with a 95% probability were denoted by different letters (A, B, C, D and E) in Table III. The letter A indicates the composites with the best values for a specific property, and the letter E indicates the composites with the lowest values for a specific property. Composites with 5% CNF and a PVA carrier system and 10% CNF showed improved tensile properties compared to neat PE samples. When 5% CNF in the PVA carrier system is compared with 10% CNF (without PVA), it seems they are not significantly different, but in terms of costs and processing (rheological properties), 5% CNF with the PVA carrier system is preferred. Table III also exhibits flexural properties of the composites. The flexure strength of neat PE is 16.2 MPa, and incorporation of CNF significantly increased flexural strength due to restricted chain mobility (20% increases with 10 wt % CNF content). The flexural modulus of elasticity (FMOE) of CNF composites was higher than that of the neat PE, and increased with increasing CNF loading. The FMOE increased up to 45% with 10 wt % CNF, where it reached a maximum value of 0.7 GPa. Similar to tensile properties, there was no significant difference between 5% CNF with PVA carrier and 10% CNF in terms of flexural properties. The Izod impact strength of the composites, reported in Table III, decreased with incorporation of CNF with the PVA carrier system. Izod impact strength decreased from 149 J/m for the neat PE to 60 J/m for 10 wt % CNF composite. The decrease in impact strength is a common trend according to previous research results for cellulose

Table III. Mechanical Properties and MFI of PE, PE+PVA, and CNF Composites

Samples	PE	PE + PVA	1%CNF	2.5% CNF	5% CNF	10%CNF
TS (MPa)	13.9 (0.3) D	14.6 (0.2) C	14.7 (0.2) BC	15.3 (0.8) B	17.4 (2.4) A	16.8 (0.3) A
TMOE (GPa)	0.8 (0.02) D	0.9 (0.04) C	1.0 (0.05) BC	1.1 (0.07) AB	1.1 (0.09) A	1.1 (0.03) A
IS (J/m)	149 (18) A	136 (16) A	104 (7) B	85 (11) C	73 (4) CD	60 (4) D
FS (MPa)	16.2 (0.3) E	16.8 (0.5) DE	17.2 (0.9) CD	17.7 (3.3) BC	18.2 (3.7) B	19.5 (0.6) A
FMOE (GPa)	0.5 (0.06) D	0.5 (0.02) C	0.5 (0.04) C	0.6 (0.02) BC	0.6 (0.02) AB	0.7 (0.04) A
MFI (g/10 min)	4.7 (0.1) A	4.6 (0.1) A	4.7 (0.1) A	4.6 (0.3) A	4.1 (0.1) B	3.9 (0.1) B

Parenthesis indicates standard deviation. The same letters indicate no statistical difference between properties of composites and those around it.
TS: Tensile Strength, FS: Flexural Strength; IS: Impact Strength, FMOE: Flexural modulus of elasticity, TMOE: Tensile modulus of elasticity and MFI: Melt flow index.

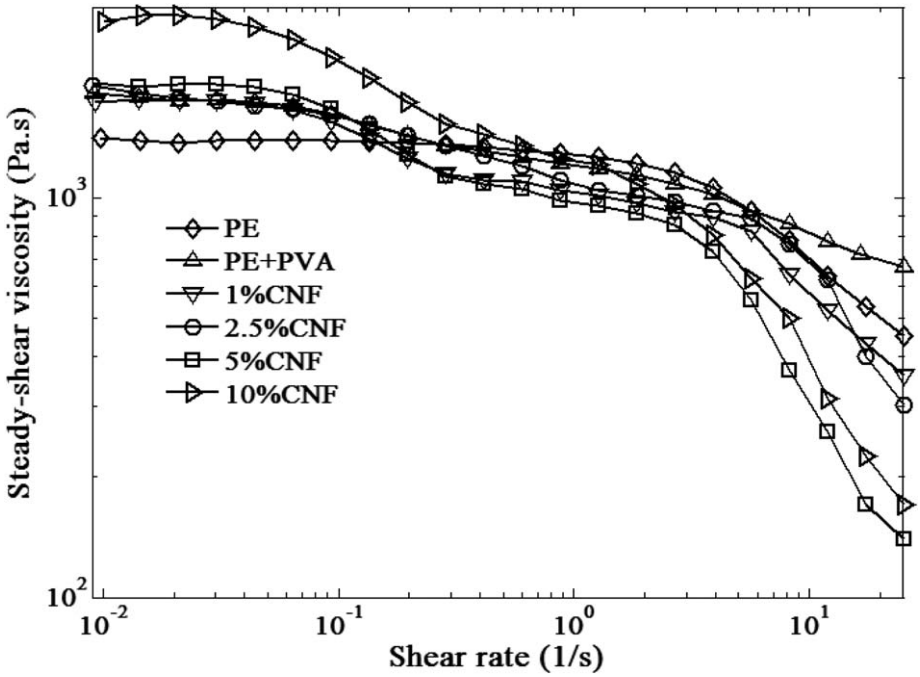

Figure 2. Steady state shear viscosity of the melt samples as a function of shear rate at 190°C.

nanofibrils and other nanomaterials.[21,45,46] The increasing CNF content only increases the interfacial regions which can cause crack propagation.[21,35,47] Interfacial bonding between CNF and PE reported in the electron microscopy section of this paper tends to support this concept.

Rheological Properties

Figure 2 depicts the variation of melt viscosity with shear rate at 190°C for the neat PE and composites. All of the PE composites behaved as pseudo-plastic fluids. Shear viscosity increased with increasing CNF content. The pseudo-plastic behavior was more pronounced as the CNF content increased. Increase in viscosity of PE after inclusion of CNF can be attributed to the creation of an entangled network of the flexible CNFs. Such network is known to suppress the deformability of polymer melt.[48,49] Shear thinning behavior was observed for all cases, with a Newtonian fluid plateau at low shear rates, shown in Figure 2. For the composite samples with 5 and 10 wt % CNF, the plateau at high shear rates was not observed in the applied shear rate range, which may indicate that the shear rate is not high enough for the microstructure in these samples to break down. Compared to neat PE, the shear viscosities at shear rate 0.01 ($\eta_{0.01}$) for 5 wt % CNF with the PVA carrier system and 10 wt % CNF are 35% and 95% higher, respectively.

The elastic moduli (G') of neat PE and the composites are shown in Figure 3. Due to intrinsic rigidity of CNF, the elastic moduli of composites were higher than the neat PE modulus. This behavior can be explained by the fact that filler particles

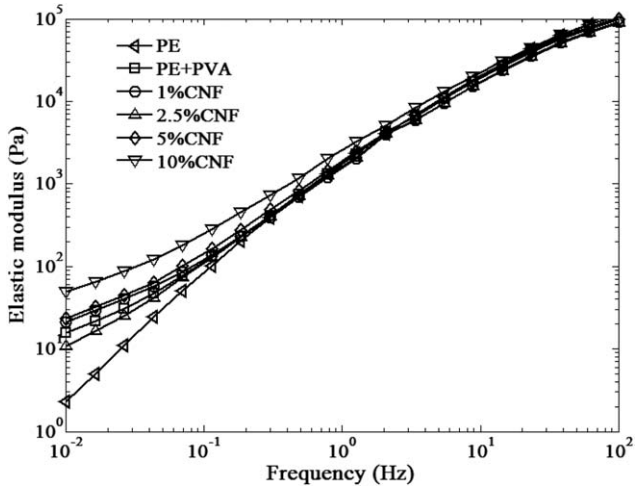

Figure 3. Storage modulus of the melt samples as a function of frequency at 190°C.

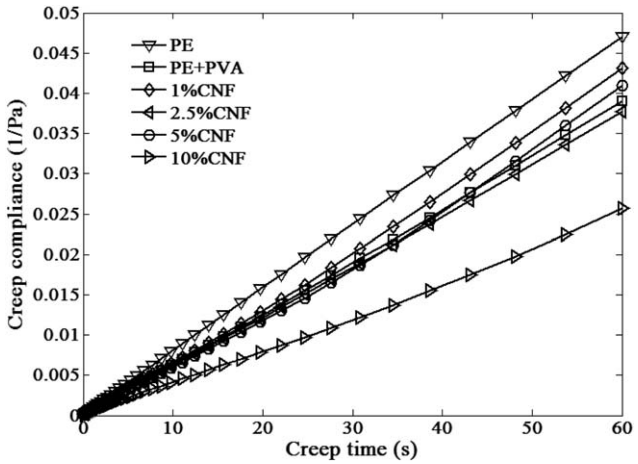

Figure 4. Melt creep compliance of for neat PE, PVA, CNF, and composites at 190°C.

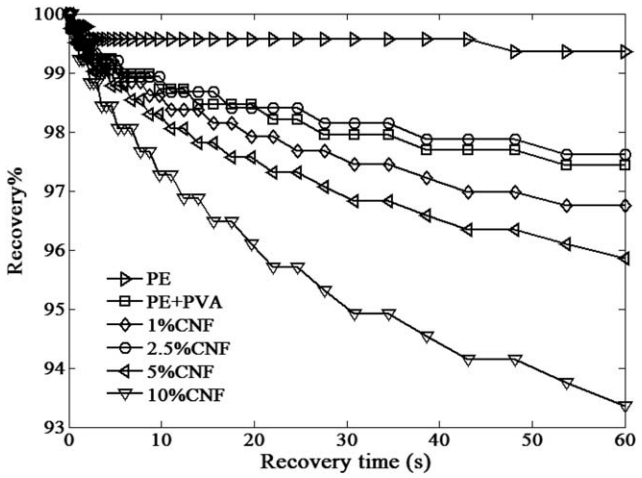

Figure 5. Melt recovery of for neat PE, PVA, CNF, and composites at 190°C.

restrict deformation.[36,49] The slope of the G' curves decreased with increasing amounts of CNF, and the decrease in the slopes of elastic modulus for the composites compared to neat PE can be explained by the microstructural changes of the polymer matrix with the incorporation of CNF.[36,48,49]

At low frequencies, G′ increased with increased CNF loading. For comparison, at $\omega = 0.1$, G′ of 5 wt % CNF with PVA and 10 wt % CNF were 68% and 190% greater than G' of neat PE, respectively. It is also evident from Figure 3 that PE/CNF composites undergo a transition from liquid-like to solid-like viscoelasticity with increased CNF loading at low frequency. In contrast, the effect of CNF on the rheological behavior is relatively weak at high frequencies, suggesting that CNF has a substantial influence on large-scale polymer chain relaxations but has little effect on short-range motion of polymer chains.[36,50] Table III shows the MFI values for the PE and CNF composites. The MFI value of the neat PE was 4.7 g/10 min., decreasing to 3.9 g/10 min. with 10 wt % CNF content. In general, low MFI, poor fluidity, and high viscosity are the reason for difficult processing of natural fiber-based composites by injection molding. The tendency for the melt viscosity to vary was similar to the MFI variation.[36]

Creep recovery tests are used to evaluate polymer melt elasticity, and some researchers previously reported creep recovery of

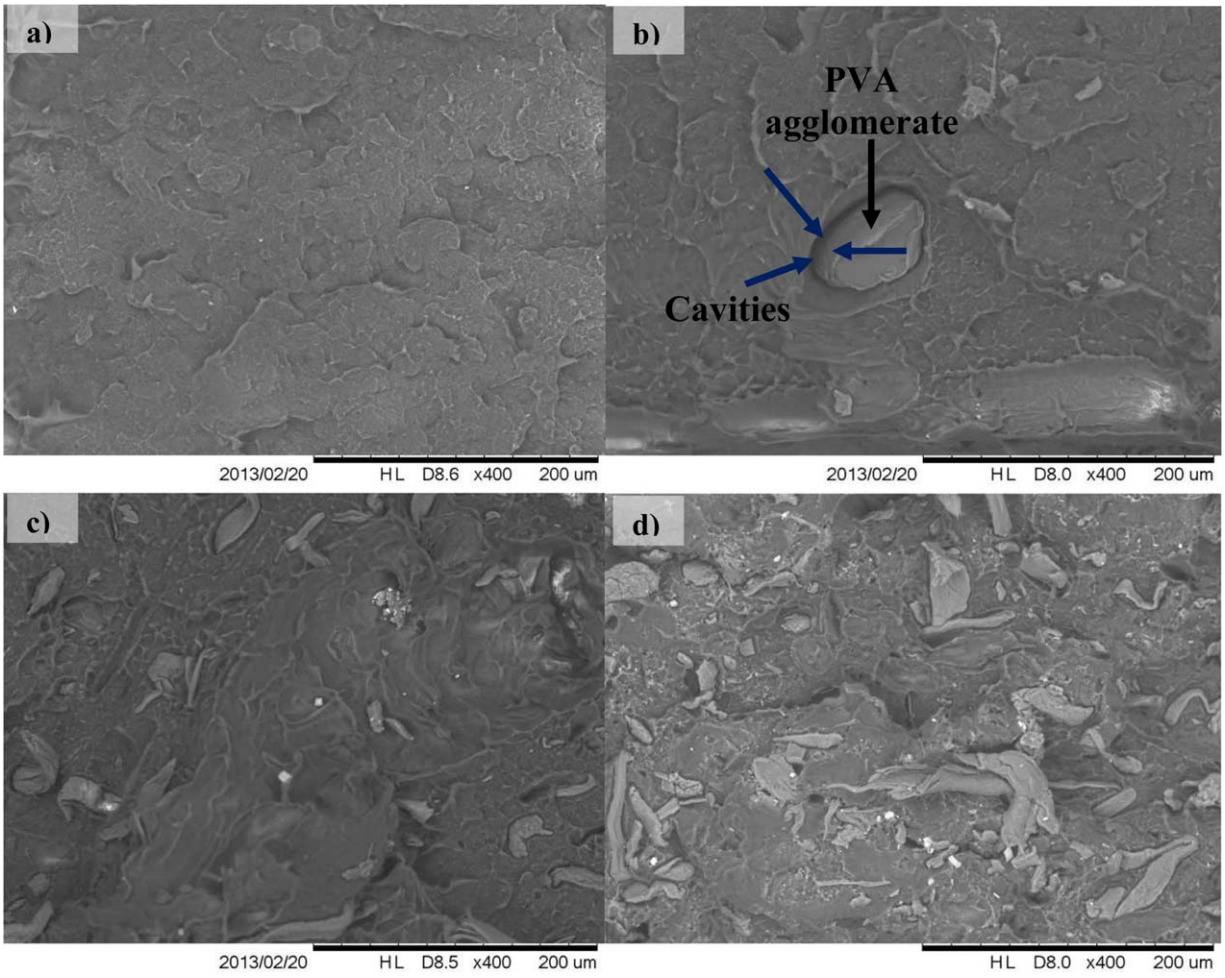

Figure 6. Overview of fractured composite surfaces: (a) neat PE, (b) PE+PVA (c) 5%CNF with PVA carrier system and (d) 10% CNF filler loading. [Color figure can be viewed in the online issue, which is available at wileyonlinelibrary.com.]

different PE samples using a rheometer in rotational mode.[51–53] In creep recovery tests, a constant stress was applied to the polymer melt for 60 s and then removed. The variation of melt creep compliance versus time is plotted in Figure 4. The observed decrease in creep compliance with the incorporation of CNF was attributed to the hindrance of chain movement by the CNF. Compared with neat PE, creep compliance at 60 s decreased by about 13% and 45% for the composites with 5 wt % CNF with PVA and 10 wt % CNF, respectively. In recovery mode, an applied strain partially recovers because of the elastic nature of polymers.[51] The results of melt recovery measurements with neat PE and CNF composites are shown in Figure 5. In general, the addition of CNF to PE increased the recoverable structure of the composites.

Morphological Properties

SEM micrographs of the impact fractured surfaces of the PE, PE + PVA, and CNF composites are presented in Figure 6. The aim was to investigate whether any CNF aggregates were visible in the impact fracture surfaces. The micrograph of PE + PVA exhibits PVA phases clustered together forming individual agglomerates with irregular shapes and sizes as well as cavities formed because of the detachment of the PVA agglomerate from the PE matrix. The agglomerates and cavities are evidence of increased interfacial tension and phase separation between the PVA and PE components.[54]

The micrographs of 5 wt % CNF with PVA and 10 wt % CNF showed evidence of aggregation of CNF fibers and generally poor adhesion between the CNF surface and the PE matrix. The cavities and agglomerates were much smaller in the 5 wt % CNF with PVA than in the 10 wt % CNF because partial hydrolyzed PVA interacted with the hydrophilic surfaces of cellulose, and the residual vinyl acetate groups with hydrophobic PE. Like the Bondeson and Oksman study, the CNFs appeared to be preferably located in the PVA phase because of greater compatibility with PVA than PE.[33] Weak interfaces (cavities and agglomerates) appeared in all composites in Figure 6. Propagation of cracks mainly around the interfaces indicated weak interfacial bonding and the presence of plastic deformation mechanisms. This crack propagation mechanism is believed to be the reason for the relatively lower impact properties for PVA and CNF-filled composites.[55]

CONCLUSIONS

This study demonstrated that the melt processing of CNF-based nanocomposites with better dispersion and good mechanical properties can be successfully developed using a novel carrier system (PVA), which creates compatibility between the CNF and hydrophobic polymer matrix (PE). Thermal stability and rheological properties of PE and composites with various CNF loadings with a PVA carrier system were also studied in this work. The thermal stability of the composites decreased slightly as CNF content increased because of the lower thermal stability of CNF compared to the neat PE. Shear viscosity increased with CNF content. The melt creep compliance decreased with the incorporation of CNF. The addition of CNF to the system also increased the melt recoverable structure of the composites. Overall, advantages of the carrier system include the use of wet, high solid CNF suspension in combination with a conventional melt blending process that has been optimized to produce enhanced PE-based nanocomposites. No pre-drying of the CNF was required before the compounding, which can save process time and money. The commercial application for this method would be in glass fiber and inorganic-filled PE composites such as in packaging, automobile applications (side panels, dashboard etc), and related consumer goods.

ACKNOWLEDGMENTS

The authors thank Chris West and Alex Nash for all of their hard work for production, characterization and material properties of the polymer nanocomposites. The authors also thank U.S. Army Engineer Research and Development Center project 912HZ-07-2-0013 and the Maine Agricultural and Forest Experiment Station (MAFES) project ME09615-08M. Permission to publish was granted by Director, Geotechnical and Structures Laboratory, at the U.S. Army Engineer Research and Development Center.

REFERENCES

1. Ben Azouz, K.; Ramires, E. C.; den Fonteyne, W. K.; Kissi, N. E.; Dufresne, A. *ACS Macro Lett.* **2012**, *1*, 236.
2. Lee, S. H.; Teramoto, Y.; Endo, T. *Compos. Part A: Appl. Sci. Manuf.* **2011**, *42*, 151.
3. Bahar, E.; Ucar, N.; Onen, A.; Wang, Y.; Oksuz, M.; Ayaz, O.; Ucar, M.; Demir, A. *J. Appl. Polym. Sci.* **2012**, *125*, 2882.
4. Siro, I.; Plackett, D. *Cellulose* **2010**, *17*, 459.
5. Eichhorn, S. J.; Dufresne, A.; Arunguren, M.; Marcovich, N. E.; Capadona, J. R.; Rowan, S. J.; Weder, C.; Thielemans, W.; Roman, M.; Renneckar, S.; Gindl, W.; Viegel, S.; Keckes, J.; Yano, H.; Abe, K.; Nogi, M.; Nakagaito, A. N.; Mangalam, A.; Simonsen, J.; Benight, A. S.; Bismarck, A.; Berglund, L. A.; Peijs, T. *J. Mater. Sci.* **2010**, *36*, 2107.
6. Moon, R. J.; Martini, A.; Nairn, J.; Simonsen, J.; Youngblood, J. *Chem. Soc. Rev.* **2011**, *40*, 3941.
7. Duran, N.; Lemes, A. P.; Seabra, A. B. *Recent Pat. Nanotechnol.* **2012**, *6*, 16.
8. Charreau, H.; Foresti, M. L.; Vazques, A. *Recent Pat. Nanotechnol.* **2013**, *7*, 56.
9. Cherian, B. M.; Leao, A. L.; de Souza, S. F.; Thomas, S.; Pothan, L. A.; Kottaisamy, M. Cellulose Nanocomposites for High-Performance Applications. In Cellulose Fibers: Bio-and Nano-Polymer Composites; Kalia, S., Kaith, B. S., Kaur, I., Eds.; Springer: New York, **2011**; p 539.
10. Dufresne, A. **2013**. Nanocellulose: From Nature to High Performance Tailored Materials. Göttingen, Germany: De Gruyter.
11. Pasquini, D.; de Morais Teixeire, E.; da Silva Curvelo, A. A.; Belgacem, M. N.; Dufresne, A. *Compos. Sci. Technol.* **2008**, *68*, 193.
12. Pandey, J. K.; Lee, S.; Kim, H.-S.; Takagi, H.; Lee, C. S.; Ahn, S. H. **2012**. *J. Appl. Polym. Sci. 125*, E651.

13. Zammarano, M.; Maupin, P. H.; Sung, L. P.; Gilman, J. W.; McCarthy, E. D.; Kim, Y. S.; Fox, D. M. *ACS Nano* **2011**, *5*, 3391.
14. de Menezes, A. J.; Siqueira, G.; Curvelo, A. A. S.; Dufrense, A. *Polymer* **2009**, *50*, 4552.
15. Kelly, J. Nanocomposites Incorporating Cellulose Nanocrystals with Potential Applications in Lithium Ion Batteries. Master of Science. Oregon State University: Oregon, **2011**, p 1.
16. Wang, B.; Sain, M. *Polym. Int.* **2007**, *56*, 538.
17. Wang, B.; Sain, M. *Compos. Sci. Technol.* **2007**, *67*, 2521.
18. Miyazaki, K.; Hamadate, M.; Terano, M.; Nakatani, H. *J. Appl. Polym. Sci.* **2012**, *128*, 915.
19. Kiziltas, A.; Han, Y.; Gardner, D. J.; and Nader, J. W. Development of a Carrier System for Cellulose Nanofibrils (CN) in Polypropylene Composites. Society of Wood Science and Technolog, Proceedings of the International Convention. Geneva: Switzerland, **2010**; p 1.
20. Kiziltas, A.; Han, Y.; Gardner, D. J.; Neivandt, D.; Rushing, T. S.; Nader, J. W. Funtionlized carrier systems for cellulose nanofibrils designed for polymer composites. TAPPI International Confrence on Nanotechnology for Renewable Materials. Arlington, VA, **2011**.
21. Yang, H. S.; Gardner, D. J. *Wood Fiber Sci.* **2011**, *43*, 143.
22. Yang, H. S.; Gardner, D. J. *Wood Fiber Sci.* **2011**, *43*, 215.
23. Yang, H. S.; Gardner, D. J.; Nader, J. W. *Compos. Part A: Appl. Sci. Manuf.* **2011**, *42*, 2028.
24. Yang, H. S.; Gardner, D. J.; Nader, J. W. *J. Therm. Anal. Calorim.* **2011**, *103*, 1007.
25. Yang, H. S.; Gardner, D. J.; Nader, J. W. *J. Appl. Polym. Sci.* **2013**, *128*, 3064.
26. Yang, H. S.; Kiziltas, A.; Gardner, D. J. *J. Therm. Anal. Calorim.* **2013**, *113*, 673.
27. Ljunberg, N.; Cavaille, J. Y.; Heux, L. *Polymer* **2006**, *47*, 6285.
28. Ljungberg, N.; Bonin, C.; Bortolussi, F.; Boisson, C.; Heux, L.; Cavaille, J. Y. *Biomacromolecules* **2005**, *6*, 2732.
29. Wu, Y.; Zhou, D. G.; Wang, S.; Zhang, Y. *BioResources* **2009**, *4*, 1487.
30. Ayaz, O.; Ucar, N.; Bahar, E.; Oksuz, M.; Ucar, M.; Onen, A.; Demir, A.; Wang, Y. Production And Analysis Of Composite Nanofiber And Heat Applied Nanofiber. 2011 International Congress of Innovative Textiles, Icontex: İstanbul, Turkey, **2011**; p 1.
31. Agarwal, U. P.; Sabo, R.; Reiner, R. S.; Clemons, C. M.; Rudie, A. W. *Appl. Spectrosc.* **2012**, *66*, 750.
32. Soulestin, J.; Quievy, N.; Sclavons, M.; Devaux, J. *Polym. Eng. Sci.* **2007**, *47*, 467.
33. Bondeson, D.; Oksman, K. *Compos. Part A-Appl S* **2007**, *38*, 2486.
34. Aydemir, D.; Kiziltas, A.; Erbas Kiziltas, E.; Gardner, D. J.; Gunduz, G. *Compos. Part B Eng.* **2015**, *68*, 414.
35. Ozen, E.; Kiziltas, A.; Erbas Kiziltas, E.; Gardner, D. J. *Polym. Compos.* **2013**, *34*, 544.
36. Kiziltas, A.; Nazari, B.; Gardner, D. J.; Bousfield, D. W. *Polym. Eng. Sci.* **2014**, *54*, 739.
37. Aydemir, D.; Kiziltas, A.; Gardner, D. J.; Han, Y.; Gunduz, G. *Int. J. Polym. Anal. Characterization* **2015**, *20*, 231.
38. JMP Statistical Discovery Software, Version 8. SAS Institute, Inc.: Cary, NC, **2008**.
39. Frone, A. N.; Panaitescu, D. M.; Donescu, D.; Spataru, C. I.; Radovici, C.; Trusca, R.; Somoghi, R. *BioResources* **2011**, *6*, 487.
40. Qua, E. H.; Hornsby, P. R.; Sharma, H. S. S.; Lyons, G.; McCall, R. D. *J. Appl. Polym. Sci.* **2009**, *113*, 2238.
41. Lee, S. Y.; Mohan, D. J.; Kang, I. A.; Doh, G. H.; Lee, S.; Han, S. O. *Fiber. Polym.* **2009**, *10*, 77.
42. Kiziltas, A.; Gardner, D. J.; Han, Y.; Yang, H. S. *Wood Fiber Sci.* **2010**, *42*, 165.
43. Kakroodi, A. R.; Cheng, S.; Sain, M.; Asiri, A. *J. Nanomater.* **2014**, *7*, 903498, DOI: 10.1155/2014/903498.
44. Alemdar, A.; Sain, M. *Compos. Sci. Technol.* **2008**, *68*, 557.
45. Zhang, J.; Wang, X.; Lu, L.; Li, D.; Yang, X. *J. Appl. Polym. Sci.* **2003**, *87*, 381.
46. Zhang, Q. X.; Yu, Z. Z.; Xie, X. L.; Mai, Y. W. *Polymer* **2004**, *45*, 5985.
47. Zaini, M. J.; Fuad, M. Y. A.; Ismail, Z.; Mansor, M. S.; Mustafah, J. *Polym. Int.* **1996**, *40*, 51.
48. Gonzalez-Sanchez, C.; Fonseca-Valero, C.; Ochoa-Mendoza, A; Garriga-Meco, A.; Rodriguez-Hurtado *Compos. Part A: Appl. Sci. Manuf.* **2011**, *42*, 1075.
49. Shumigin, D.; Tarasova, E.; Krumme, A.; Meier, P. *Mater. Sci. (Medziagotyra)* **2011**, *17*, 32.
50. Wang, M.; Wang, W.; Liu, T.; Zhang, W. D. *Compos. Sci. Technol.* **2008**, *68*, 2498.
51. Riahinezhad, M.; Ghasemi, I.; Karrabi, M.; Azizi, H. *Polym. Compos.* **2010**, *31*, 1808.
52. Gabriel, C.; Kaschta, J. *Rheol. Acta* **1998**, *37*, 358.
53. Gabriel, C.; Munstedt, H. *Rheol. Acta* **1999**, *38*, 393.
54. Ismail, H.; Nordin, R.; Ahmad, Z.; Rashid, A. *Iran. Polym. J.* **2010**, *19*, 297.
55. McHenry, E.; Stachurski, H. Z. *Compos. Part A* **2003**, *34*, 171.